The 2009 IEEE/RSJ International Conference on
Intelligent Robots and Systems
October 11-15, 2009 St. Louis, USA

A Design of the Electromagnetic Driver for the "Internal Force-Static Friction" Capsubot

Gang Su, Cheng Zhang, Renjia Tan, Hongyi Li, Member, IEEE

***Abstract*—A capsule robot that moves utilizing the internal force between the shell and the sliding mass and the friction between the shell and the environment is named "internal force-static friction" capsubot. The new driving mode is used in the active gastrointestinal examination robot system, which is a novel and meaningful attempt. In this paper, for the operation mechanism and movement characteristics of capsubot, a new type of electromagnetic driver has been designed. The driver is optimized and analyzed by magnetic circuit method and finite element method. Then we manufacture the prototype of the capsubot. The driver has big output power, a small size and a high weight proportion of the sliding mass and the shell, which has been proved by the experiment. The speed on the table is 45.8mm/s.**

I. INTRODUCTION

A micro robot that works in human gastrointestinal tract has been a research focus for many years. Designing a driving mode that adapt to the special environment in the gastrointestinal tract under the condition of wireless energy supplying is the main difficulty. Many researchers focus on bionic driving; screw driving, paddle driving and foot driving and many other driving mode [1-4]. The capsubot that moves utilizing the internal force between the shell and the sliding mass and the friction between the shell and the environment is used in the active gastrointestinal examination robot system, which is a novel and meaningful attempt. There are no wheels, pedrails and legs on the body, which is no harm to the human body. The robot has a simple structure. We can make the capsubot move forward or backward and accelerate or decelerate by means of controlling the internal force [5]. The internal forces of the entire robot system play a major role in driving performance.

Now among those widely used driving modes, piezoelectricity drivers have large output force and short response time but small output displacement and high driving voltage, while shape memory alloy drivers has large displacement but long response time [6]. The electromagnetic driver has low driving voltage, is easy to control and easy to design the output force-displacement relation, which makes it applicable to the driving mode of "internal force-static friction" capsubot. There is almost no such linear motor that has the diameter below 10mm and is suitable for the "internal force-static friction" capsubot. Therefore, we designed an electromagnetic driver by ourselves.

The whole structure of the driver is designed according to the requirement in part 2. In part 3 there is parameter optimization by the magnetic circuit method. We analyze the output of the driver detailedly by the finite element method in part 4. In the end we produce the prototype and do some experiment and analysis .

Manuscript received February. 26, 2009.

Gang Su, Cheng Zhang, Renjia Tan and Hongyi Li are with the State Key Laboratory of Robotics, Shenyang Institute, Chinese Academy of Sciences, 114 Nanta Street, Dongling District, Shenyang 110016, China

Phone: 86-024-23970527; fax: 86-024-23970021; e-mail: hli@sia.cn.

II. THE ROBOT'S OPERATION PRINCIPLE AND THE DRIVER'S STRUCTURE

A. The Robot's Operation Principle

The capsubot can be divided into two parts: the shell and the sliding mass according to their function when the capsubot moves. To move the capsubot forward, the required motion consists of four steps (Figure 1):

1) Large backward accelerated motion of the sliding mass, forward accelerated motion of the shell.

2) Small backward decelerated motion of the sliding mass, forward decelerated motion of the shell.

3) Small backward decelerated motion of the sliding mass, the shell remains stationary.

4) Forward slow motion of the sliding mass, the shell remains stationary.

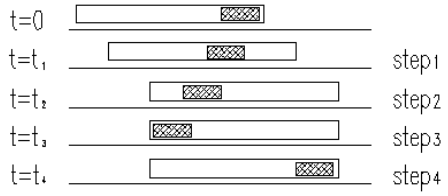

Figure 1. One movement cycle of the capsubot

According to the preliminary studies the capsubot needs a bigger output force in both ends of the sliding route with the restriction of the power consumption. Increasing the weight proportion of the sliding mass and the shell makes the moving step length of the capsubot larger. Increasing the proportion of the internal force and the static friction makes the moving frequency of capsubot larger [5].

B. The Driver's Structure

The driver needs to have the following characteristics according to the analysis above:

The capsubot needs a bigger output force in both ends of the sliding route, which makes the driving more efficient.

The rated power consumption needs to be lower than 0.2W with the restriction of the wireless power supplying in human body [4].

The output force of the driver needs to increase to maximum.

The weight proportion of the sliding mass and the shell needs to increase to maximum.

We improved the basic principles of the traditional voice coil motor (VCM) to meet the requirements above. VCM belongs to moving-coil linear oscillatory motor, the structure of which is shown in Figure 2. VCM uses the coil as the moving part that is lighter to achieve a high vibration frequency. On the contrast, the capsubot need a heavy moving part. Therefore, the coil is used as the fixed part to attach to the shell and the sliding mass is used as the moving part, which maximize the weight proportion of the sliding mass and the shell. Increasing the magnetic flux density is the most efficient method to improve output force according to $F = BIL$ under the condition of a certain current and resistance. The magnetic leakage at both of the two ends and the non-working air gap seriously impacts the utilization of the permanent magnet for the structure of the VCM, when the magnetic flux density increases at the working air gap. We use several VCM series in the paper. The arrangement of the permanent magnet and the magnetic circuit are shown in Figure 3. The structure almost eliminates the magnetic flux leakage on the outside of the permanent magnet cylinder. The magnetic flux creates the magnetic coagulation effect at the outside of the magnetic gaskets. Time-sharing power supplying is adopted to avoid the energy loss at the position of low magnetic flux density.

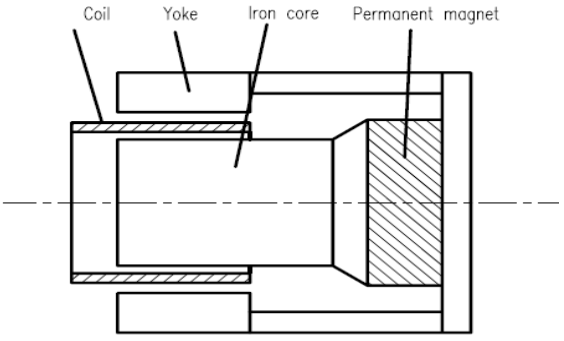

Figure 2. The structure of the VCM

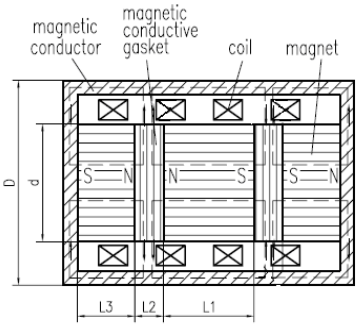

Figure 3. The structure of the driver

We call the four coils 1, 2, 3and4 from left to right in Figure 3. The relative positions of four coils are fixed. In the beginning the coils are placed in the right of the air gap, and then coil 2 and 4 lie in the outside air gap of magnetic conductive gasket. Because of the opposite direction of magnetic induction intensity in the air gap, the current in coil 2 and 4 goes in the opposite direction, which makes the two coils have electromagnetic force right. Then four coils glide right. When coils 2 and 4 go out of the outside air gap of magnetic conductive gasket, coils 1 and 3 are just in this field and have the current. Then the coils go right until coils 1 and 3 go out of the outside air gap of magnetic conductive gasket entirely. Now the coils are in the right end of the air gap. When the sequence and direction of electricity supply of the coils are changed, the coils go back to the start point. This is a cycle. Because of the magnetic leakage, there is still electromagnetic force on the coils when they move out of the air gap around the gasket, so the cycle can run smoothly.

III. MATERIAL SELECTION AND STRUCTURAL PARAMETER OPTIMIZATION

A. Material Selection

Magnetic materials selection and magnetic circuit planning are the most important factor to affect the capability of the electromagnetic driver. The standard of judging the capability of permanent magnetic material contains residual magnetic induction intensity Br, maximum energy product BH, coercivity Hc, residual magnetic induction intensity temperature coefficient α_{Br}, coercivity temperature coefficient α_{Hr} and curie point etc. In the field of the micro motor, most people pay attention to the alnico and the rare earth permanent magnet materials because of their big residual magnetic induction intensity. The alnico has higher temperature stability and Curie point, while the rare earth has higher coercivity. Because the driver is designed for the capsubot, the working temperature of the driver is lower and relatively steady and magnet has higher coercivity for magnetic coagulation effect. Therefore, the rare

earth permanent magnet material is more suitable. We choose NdFeB for hard magnet and pure iron, which has higher saturation magnetic induction intensity, magnetic permeability and good mechanical properties for soft magnet.

B. Variable Definition

In physics we know

$$F = \int_V (J \times B) dV \tag{1}$$

Where

F —Electromagnetic force

J —Current density

B —Magnetic induction intensity

V —Solution domain

The main structural parameters of driver are magnetic conductor external diameter D, magnetic conductive objects thickness, magnet and gasket diameter d, magnet thickness L_1, L_3 and gasket thickness L_2, which are shown in Figure 1. Magnetic conductor external diameter D is set to 0.7cm and output journey is set to 0.2cm because of the volume of capsubot. To make magnetic conductor have better Stiffness and magnetic flux, the thickness of magnetic conductor is set to 0.05cm, and then the length is $(0.1 + L_1 + 2 \times L_2 + 2 \times L_3)$ cm. To sum up, there are three main variables, gasket thickness, gasket diameter and magnet thickness.

C. Parameter Optimization

The whole driver is parameterized by the way of magnetic circuit method for the best drive performance. These parameters are helpful to the accurate finite element analysis. The combination of parameters is determined by the impact of variable.

We set magnetic flux density as average in integral domain and magnetic line is perpendicular to the platform of the gasket for simplified according to (1). The maximum output force formula of the driver is simplified to $F = |J| \times |B| \times V$. Where "| |" stands for modulus. The expressions of parameters are:

$$|J| = \sqrt{\frac{p}{4V\rho r^2}} \tag{2}$$

Where

P —Power

V —Integral domain

ρ —Resistivity of lead

r —Radius of lead

$$V = \pi L_2 (0.6^2 - d^2) \times 10^{-6} / 8 \tag{3}$$

From circuit Ampere's law and magnetic Ohm's law

$$\sum F = H_m l_m + \delta H_\delta = 0 \tag{4}$$

$$F = \phi \times 1/G = \delta H_\delta \tag{5}$$

Where

F —Magnetic Potential

δ —Air gap thickness

G —Magnetic permeability

Ignoring Magnetic leakage we have

$$\phi = -H_m l_m G \tag{6}$$

Demagnetization curve of NdFeB meets approximativel $B_m = 1.44 + 1.31 \times 10^{-6} H_m$. According to the principle of constant flux $\phi = \phi_m$, H_m is expressed as a function of ϕ

$$H_m = (\frac{3\phi}{\pi d^2} \times 10^4 - 1.1) \times 10^6 \tag{7}$$

Substitute to $\phi = H_m l_m G$ is

$$\phi = \frac{1.44\pi d^2 L_3 G}{4 \times 10^4 L_3 G + 1.31 \times 10^{-4} \pi d^2} \tag{8}$$

If S is the average cross-sectional area of airgap

$$S = (0.6 + d)\pi L_2 \times 10^{-4} / 4 \tag{9}$$

The magnetic permeability between two concentric cylinders is :

$$G = \frac{2\pi\mu_0 L}{ln\frac{2C + d_r}{d_r}} \tag{10}$$

Where

L —The height of cylinder. In the driver it is gasket thickness $L_2 / 2$.

μ_0 —Vacuum magnetic permeability

C —Air gap thickness

d_r —The diameter of cylinder inside. In the driver it is d.

The result of simplification is

$$G = \frac{\pi\mu_0 L_2}{ln\frac{0.6}{d}} \tag{11}$$

According to magnetic flux density formula $B = \phi / S$, we have the average magnetic flux density.

Substitute to $F = |J| \times |B| \times V = J \times \phi \times V / S$

We have

$$F = 21.1\sqrt{\frac{L_2(0.6-d)}{0.6+d}} \bullet \frac{L_3 d^2}{4.1d^2 \ln\frac{0.6}{d} + 15.6L_2L_3} \quad (12)$$

Because the parameter of lead and power are most restricted by electrical interface, we set power is 0.2w and the diameter of lead is 0.06mm. The structural parameters on the impact of the output electromagnetic force are shown as Figure 4, 5, 6.

From the figures above, when F is maximum, L_2 is 0.08cm, d is 0.53cm. The longer the magnet, the larger the outputs force. When the length of magnet is beyond 0.15cm, the effect on the output force becomes smaller. Then we choose the structural parameter as below:

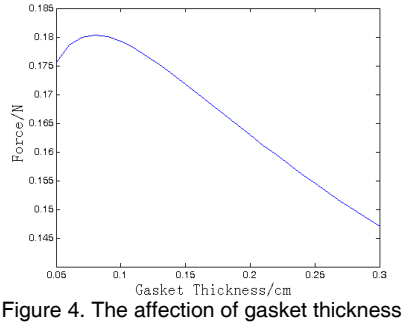

Figure 4. The affection of gasket thickness

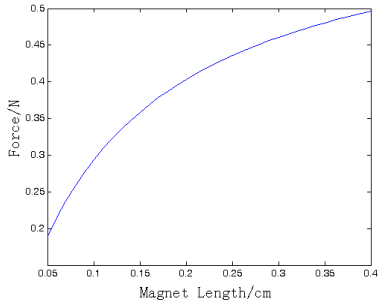

Figure 5. The affection of magnet length

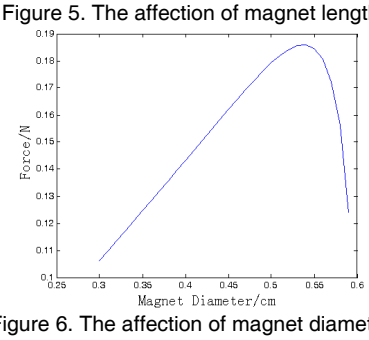

Figure 6. The affection of magnet diameter

Magnet diameter: 0.5cm

Magnet thickness on one side: 0.2cm (increase extra 0.05cm for moving)

Middle magnet thickness: 0.3cm

Magnetic conductive gasket thickness: 0.1cm

IV. Finite Element Analysis

We get the distribution of magnetic induction intensity and the curve of magnetic induction intensity in gasket by finite element analysis, which are shown in Figure 7 and 8. The magnetic induction intensity in the magnet is about 0.9T by analysis. This point is in the field where energy product is large according to the characteristic curve of the magnet. Therefore the utilization of magnet is nice. The maximum of magnetic induction intensity in gasket in Figure 8 is about 2T, which is saturation value. The static output force curve of driver by calculation is shown in Figure 9. The curve is half of a journey because of symmetrical structure. The maximum is 0.29N and the minimum is 0.11N. To sum up, the materials are fully utilized and the output force is focus on both ends of the sliding route. Therefore, the structural parameter of driver is reasonable.

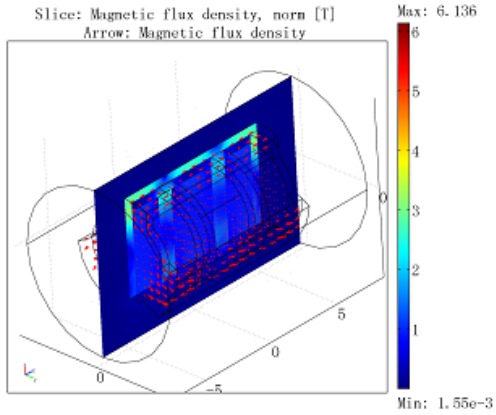

Figure 7. The distribution of magnetic induction intensity

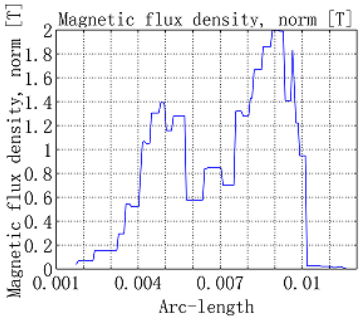

Figure 8. The curve of magnetic induction intensity in gasket

V. Overall Structural Design

The main structure of the capsubot is shown in Figure 9. The coil of the driver is attached to the shell by the bracket. There are three slots on the magnetic conductor, which makes the three claws of the bracket link to the coil closely. There are washers fixed between the coils to make the position relationship of the coils. The shell, the bracket, the coils, the washers and the covers on both two ends which are not shown in Figure 9 form the whole shell of the capsubot. The other parts of the driver are used as sliding mass, which slides in the shell by the electromagnetic force.

We produce a prototype of the capsubot according to design, which is shown in Figure 10. The pulse signal

produced by PC is used as driving source [5]. The pulse signal go through the external drive circuitry. The output of the circuitry is the control signal. The principle of the external drive circuitry is shown in Figure 11.

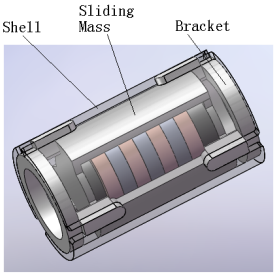

Figure 9. The main structure of the capsubot

VI. RESULT AND ANALYSIS

The resistance of each coil is 9.4Ω and the peak value of driving current is 100mA according to actual measurement. The data is measured every 0.1mm from the start point. The static output force has symmetry on the whole journey because of the symmetrical structure of the driver. The measured output force character in the former half journey and simulation result are shown in Figure 11. The maximum electromagnetic force measured is 0.245N and the minimum is 0.06N. The length of the prototype is 30mm, and the diameter is 8mm. The length of sliding mass is 10mm, the journey is 2mm, and the mass is 1.87g. The whole capsubot weighs 2.89g. On the table the max speed is 45.8mm/s, the vibration frequency is 41.6Hz and the average step is 1.1mm.

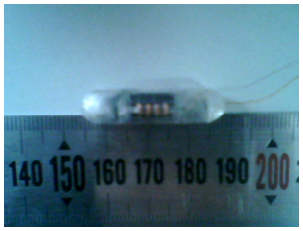

Figure 10. The prototype of the capsubot

The calculated values and the real values have the same trend in Figure 10. But the latter are 0.05N smaller than the former. There are three reasons. One is the movement gap is ignored by mesh in simulation. The other is that there is inaccuracy between coils because of the batch of enamel insulated wire, the degree of tension at enlacing and the quality of enlacing and so on. The third one is the part has errors in permitted tolerance. The first one is the major cause.

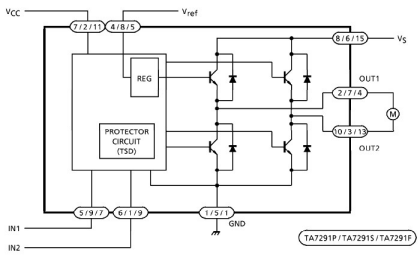

Figure 11. The principle of the external drive circuitry

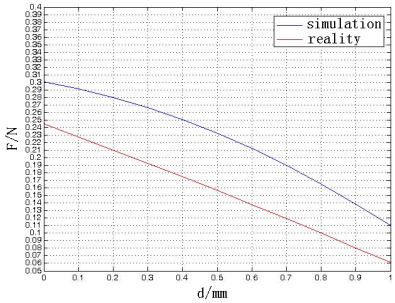

Figure 12. The output force comparison between reality and simulation

REFERENCES

[1] Sukho Park, Hyunjun Park, sungjin Park, “paddling based locomotive mechanism for capsule endoscopes,” Journal of Mechanical Scien and Technology, Vol.20, No. 7,2006Page(s): 1012-1018 .

[2] Federrico Carpi and Carlo Pappone, “Magnetic Maneuvering of Endoscopic Capsules by Means of a Robotic Navigation System”, IEEE Transaction on Biomedical Engineering, Vol. 56, No. 5, May 2009Page(s): 1482-1490.

[3] Jiwoon Kwon, Sukho Park, Byungkyn Kim and Jong-Oh Park, “Bio-material property measurement system for locomotive mechanism in gastro-intestinal tract”, proceedings of The 2005 IEEE International Conference on Robotics and Automation Barcelona, Spain, April 2005Page(s): 1303-1308.

[4] Kundong Wang, Guozheng Yan, Guanying Ma and Dongdong Ye, “An Earthworm-Like Robotic Endoscope System for Human Intestine Design, Analysis, and Experiment,” Annals of Biomedical Engineering, Vol. 37, No. 1, January 2009Page(s)210-221.

[5] H. Li, K. Furuta, and F. Chernousko, “A Pendulum-driven Cart via Internal Force and Static Friction”, Proc. of Int. Conf. Physics and Control, St. Petersburg, Russia, 2005Page(s): 15-17,

[6] G. Chen, W. Zhang, B. Peng, C. Jiang, “Research on drive principle of Micro actuators”, micro motor, 2005 /38 /01 :61-63

[7] N. Bianchi, S. Bolognani, F. Tonel, “ Design Consideration for a Tubular Linear PM Servo Motor”, EPE Journal, Vol. 11, No.3, Aug. 2001 Page(s):41-47

[8] H. Lu, J. Zhu and Y. Guo, “ A Permanent Magnet Linear Motor for Micro Robots, Power Electronics and Drives Systems, ”2005. PEDS 2005. International Conference on Volume 1, 16-18 Jan. 2006 Page(s):590 – 595

[9] Y. Suzuki, Hongyi Li. , K. Furuta, “Locomotion generation of friction board with an inclined slider, ”Decision and Control, 2007 46th IEEE Conference on12-14 Dec. 2007 Page(s):1937 - 1943

[10] K. Wang, G.Yan, “A miniature permanent magnet linear DC motor”, ELECTRIC MACHINES AND CONTROL , 2006/10/1page(s): 70-73

[11] Zongli Lin and Matthias Glauser, “Magnetically suspended balance beam with disturbances: a test rig for non-linear output regulation,” Int. J. Advanced Mechatronic Systems,Vol 1, No. 1, 2008,pp.2-9.

[12] Paul C.-P. chao and Sung-Ching Wu, “Optimal Design of Magnetic Zooming Mechanism Used in Cameras of Mobile Phones via Genetic Algorithm,” IEEE Transactions on Magnetics, Vol. 43. NO. 6. JUNE 2007, pp.2579-2581.

[13] Rahul Banik, Dong-Yeon Lee and Dae-Gab Gweon, “Optimal Design of Voice Coil Motor for Application in Active Vibration Isolation,” 4th International Conference on Electrical and Computer Engineering ICECE 2006, 19-21 December 2006, Dhaka, Bangladesh, pp.341-344.